Ecole Nationale Supérieure d'Informatique et de
Mathématiques Appliquées de Grenoble

Research Internship Report 2A

with the EDP team at the Jean Kuntzmann Laboratory,
supervised by Emmanuel Maitre and Édouard Oudet,
examined by Picard Christophe and Louissi Soad.

Optimal Transportation : Applications to Image processing

Jérémy Rouot

51 rue des Mathématiques
Campus de Saint Martin d'Hères
BP 53 - 38041 Grenoble cedex 09

June 16 - August 31, 2012
10 weeks

Contents

Section 1

Introduction

Born in France in 1781, optimal transportation theory was formalized by Monge in his memoir *Théorie des déblais et des remblais.* Originally, the issue may be conceptually described as follows

> *from a given area, called the "Déblai", how to transport the earth, considered of uniform infinitesimal thickness, to a given area, called the "Remblais", with the least amount of carriage.*

During the 20th century, the theory gathered many areas of mathematics and what was a discrete mass transfer problem was generalized to the continuous case where probability measures are involved. However, most approximation problems were too sophisticated and it was only recently that some breakthrough discoveries were made in applied mathematics including non linear optimization problems which led on many search areas such as image processing.

A grayscale image is defined by a value, the grayscale, associated to each pixel. Therefore, we can defined a probability density function ρ defined on $\mathbb{R}^d$ with compact support (with d the dimension of the image) so that $\rho(x)$ is equal to the grayscale of the pixel x. Let's consider a pair of two-dimensional images relatively close in a sense that we will explain later.

Figure 1: Initial and final two-dimensional image which can be represented by the density function $\rho(x, y) = \chi_{[a,b]}$.

We are interested in finding an interpolating movie between them namely the white-band could translate herself. One may suggest to compute the linear interpolating of these two images. However, we would simply observe a blackening and a whitening of each band which is not the rendering expected.

The idea of the optimal transportation is to define a distance between two images that we have to minimize. This may also be rephrased as a fluid mechanics problem consisting in determining minimizing geodesics which satisfy the incompressible Euler equation. Suppose our two images are two fluid flows, optimal transportation consists in moving particles along paths from the first flow to the second. This appears more convenient for visualization.
The latter problem may be solved by the Benamou-Brenier's algorithm which compute the optimal transportation between these two images. However this method seems too rough since no direction is favored. Actually, we would like to control direction paths namely compel transport to be done along a fixed direction.

Suppose we are given a sequence of one-dimensional images. For instance, let the sequence $(\rho(x,s))_s$ defined in $[0,1]$ by $\rho(x,s) = e^{-k(x-s)^2}$. A one-dimensional image may be viewed as a frame of a two-dimensional image. One may correspond to this sequence a two-dimensional image as represented in Figure 2. By this way, given two sequences of one-dimensional images,

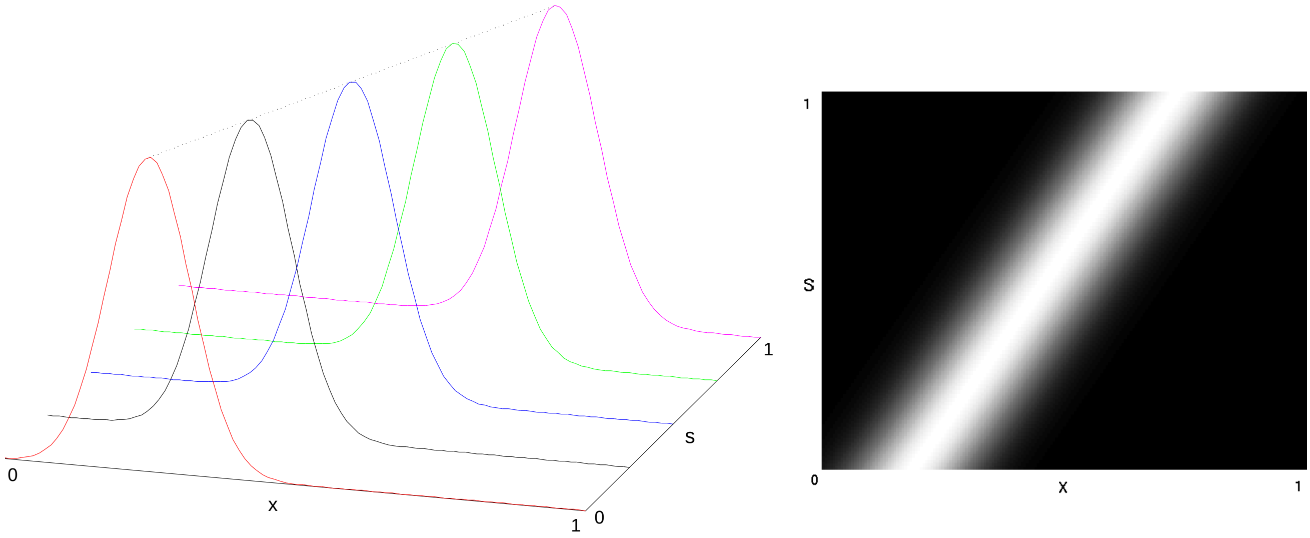

Figure 2: *Left* : Sequence of Gaussian densities. Five frames are illustrated. *Right* : The corresponding two-dimensional image.

for each frame of each sequence we could compute the optimal transportation and then obtain an interpolation which would be, *a priori*, different from the previous interpolation.

Throughout this report, we recall some basic facts about the optimal transportation theory. Namely, Monge-Kantorovich's formulation, fluid mechanics formulation and an efficient algorithm by Benamou-Brenier.

Then, following the Benamou-Brenier's formulation, we introduce a new model to determine interpolating frames and present its numerical resolution based on the Benamou-Brenier algorithm.

Finally, we discuss different methods and implementations and deal with theoretical points.

Section 2

Working environment

The Jean Kuntzmann Laboratory focuses on three research areas

- Geometry and Images,
- Deterministic models and Algorithms,
- Statistics.

I was affiliated to the EDP's team which belongs to the Deterministic and Algorithms area. The teams is composed by 37 members whose 14 researchers and engineers and 23 Post Docs, PhD students and trainees.

Optimal transportation gathers many researchers since an ANR (National Research Agency) project TOMI (Optimal Transportation and Image Multiphysics) was created on November 2011. It aims to develop models and algorithms in optimal transportation combined with

image processing.
I was supervised by Emmanuel Maitre and Édouard Oudet. I saw them about twice a week and their dedication was very substantial to lead me throughout my internship, I truly thank them for that.
I worked in a room with many PhD students. I implemented my programs using Scilab and Matlab.

Section 3

What do we know ? What are the objectives ?

3.1 Monge-Kantorovich's formulation

The framework of the Monge-Kantorovich problem is as follows. Let ρ_0 and ρ_1 two probability densities defined on $\mathbb{R}^d$ with a compact support Ω, in particular, they have an unit mass. The issue is to find a one-to-one map T from Ω to Ω which realizes the transfer of ρ_0 to ρ_1 and that we denote by $T\#\rho_0 = \rho_1$. More formally, for any $A \subset \Omega$, the mass $\rho_0(T^{-1}(A))$ has to be equal to $\rho_1(A)$. This may be written as

$$\forall A \subset \Omega, \int_{x \in A} \rho_1(x)dx = \int_{T(x) \in A} \rho_0(x)dx.$$

Thanks to the change of variable formula (with $T \in C^1$), we deduce the equation

$$\rho_0(x) = |\nabla T(x)|\rho_1(T(x)). \tag{3.1}$$

This non linear equation is difficult to solve numerically and, at first glance, existence or uniqueness of a solution is not clear. Beside, the existence of T depends on the regularity of ρ_0 and ρ_1. Due to the injectivity of T, mass can't be split in this formulation. For instance, there is no solution for $\rho_0 = \delta_x$ and $\rho_1 = \frac{1}{2}(\delta_x + \delta_y)$.

When the problem has a solution, we may think to select maps which are optimal in a suitable sense. The L^p-Kantorovich's distance defined by

$$d_p(\rho_0, \rho_1)^p = \inf_{T, T\#\rho_0=\rho_1} \int |T(x) - x|^p \rho_0(x)dx$$

compels T to respect a metric constraint. Intuitively, in the case of $p = 2$, T has to minimize the distance of the displacement of the point x to his image $T(x)$. Moreover the cost of the displacement is not the same for all points since they are affected by “a weight“ given by $\rho_0(x)$. Throughout the rest of the document, we will refer the Monge-Kantorovich problem as

$$\inf_T \{\int \frac{1}{2}|T(x) - x|^2 \rho_0(x)dx, T\#\rho_0 = \rho_1\}. \tag{3.2}$$

3.2 Benamou-Brenier's formulation

Benamou and Brenier pointed out an "Eulerian“ formulation of the optimal transportation problem. We retail steps described in [1]. They introduced a time parameter t which would make the problem more intuitive.

The idea is to construct the flow $(\rho(t, x), v(t, x))$ where $\rho(t, x)$ stands for the mass at the space point x at the time t and $v(t, x)$ stands for the velocity of particles going through x at the time t for given $\rho(t{=}0, .)$ and $\rho(t{=}1, .)$ are given. To obtain trajectories of each particle, let's denote $X(t,x)$ the position at the time t of a particle that was located at position x at $t=0$, we have to solve the ODE system

$$\frac{dX(t,x)}{dt} = v(t, X(t,x)). \tag{3.3}$$

The fluid mechanics theory shows that such a fluid verifies the linear mass-conservation equation

$$\tfrac{\partial \rho}{\partial t} + \nabla.(\rho v) = 0.$$

The optimal way to move particles according to the velocity field v is to minimize the kinetic energy

$$K(t) = \int_\Omega \frac{1}{2}\rho(t,x)|v(t,x)|^2 dx = \int_\Omega \frac{|m(t,x)|^2}{2\rho(t,x)} dx \textit{ with } m = \rho v.$$

Hence Benamou-Brenier's formulation

$$\begin{aligned} &\textit{minimise}: \int_{t=0}^{1}\int_{x\in\Omega} \frac{|m(t,x)|^2}{2\rho(t,x)} dX dt \\ &\textit{subject to}: \begin{cases} \partial_t \rho + \nabla_x . m = 0, \\ \rho(t{=}0, x) = \rho_0 \textit{ and } \rho(t{=}1, x) = \rho_1. \end{cases} \end{aligned} \tag{3.4}$$

It is shown in [5] that this formulation is equivalent to (3.2).

3.3 Benamou-Brenier's algorithm

Benamou-Brenier sets forth in [1] an augmented Lagrangian method [3] to solve problem (3.4). Let's explain the different steps of the algorithm. Let us fix $\Omega = [0,1]^d$.
We first define the associated Lagrangian $L(\phi, \rho, m)$ of (3.2)

$$\begin{aligned} L(\phi,\rho,m) &= \int_{t=0}^{1}\int_{x\in\Omega} [\frac{m^T m}{2\rho} + \phi(\partial_t \rho + \nabla_x . m)] dX dt \\ &\underset{IBP}{=} \int_{t=0}^{1}\int_{x\in\Omega} [\frac{m^T m}{2\rho} - \rho \partial_t \phi - m.\nabla_x \phi] dX dt + \underbrace{\int_{x\in\Omega} [\rho_1 \phi(t{=}1,.) - \rho_0 \phi(t{=}0,.)] dX}_{G(\phi)} \end{aligned}$$

(we force the normal velocity's component to be zero on the boundary so that $m.n = 0$ with n the normal vector).

They notice that

$$\frac{m^T m}{2\rho} = \sup_{(a,b)\in K} \{a(t,x)\rho(t,x) + b(t,x).m(t,x)\}$$

where $K = \{(a,b) \in ([0,1]\times[0,1]^d) \longrightarrow ([0,1]\times[0,1]^d) \mid a(t,x) + \frac{1}{2}|b(t,x)|^2 \leq 0\}$.
Hence, with $q = \begin{pmatrix} a \\ b \end{pmatrix}$ the dual variable of $\mu = \begin{pmatrix} \rho \\ m \end{pmatrix}$,

$$L(\phi,\rho,m) = G(\phi) + \int_{t=0}^{1}\int_{x\in\Omega}[\sup_{q\in K}\{\mu.q\} - \mu.\nabla_{t,X}\phi]dXdt$$
$$= G(\phi) + \sup_{q}\{-F(q) + < \mu, q - \nabla_{t,X}\phi >\}.$$

(F is a characteristic function of K that is $F(q) = \begin{cases} 0 \; if \; q \in K \\ +\infty \; elsewhere \end{cases}$
and $< f,g >= \int_t\int_x f(t,x)g(t,x)dxdt$).
The saddle point problem can be written as

$$-\inf_{\rho,m}\sup_{\phi} L(\phi,\rho,m) = \sup_{\rho,m}\inf_{\phi,q}\{F(q) - G(\phi) + < \mu, \nabla_{t,X}\phi - q >\}$$

In this Lagrangian, μ appears to be a Lagrange multiplier for the constraint $\nabla_{t,X}\phi - q = 0$. They define an augmented Lagrangian which is convex (easier to minimize) and it makes sure that at the optimum, the latter constraint is satisfied

$$L_r(\phi,q,\mu) = F(q) - G(\phi) + < \mu, \nabla_{t,X}\phi - q > + \tfrac{r}{2}\|\nabla_{t,X}\phi - q\|^2.$$

The equivalent saddle point problem becomes

$$\sup_{\mu}\inf_{\phi,q} L_r(\phi,q,\mu).$$

To solve this problem, three steps per iteration are performed.

1. Find ϕ^n such that : $\forall\phi, L_r(\phi^n,q^n,\mu^n) \leq L_r(\phi,q^n,\mu^n)$.
2. Find q^n such that : $\forall q, L_r(\phi^n,q^n,\mu^n) \leq L_r(\phi^n,q,\mu^n)$.
3. Update the variables : $\mu^{n+1} = \mu^n + r(\nabla_{t,X}\phi^n - q)$.

1. The first step may be solved by determining $dL_{r\phi^n}(\phi)$.

$$dL_{r\phi^n}(\phi) = -G(\phi) + < \mu^n, \nabla_{t,X}\phi > + r < \nabla_{t,X}\phi^n - q^n, \nabla_{t,X}\phi > .$$

The corresponding variational formulation for $dL_{r\phi^n}(\phi) = 0$ is

$$-r\Delta_{t,X}\phi^n = \nabla_{t,X}.(\mu^n - rq^n). \tag{3.5}$$

which is a Laplace's equation.

We choose Dirichlet boundary conditions in space and Neumann boundary conditions in time. In the latter case, by integrating by parts (ψ is a test function and n is the normal vector of $\partial([0,1]\times\Omega)$)

$$-r < \Delta_{t,X}\phi^n, \psi > = r < \nabla_{t,X}\phi^n, \nabla_{t,X}\psi > -r\int_{x\in\partial([0,1]\times\Omega)}\nabla_{t,X}\phi^n.n\psi dX \tag{3.6}$$
$$= r < \nabla_{t,X}\phi^n, \nabla_{t,X}\psi > -r\int_{x\in\Omega}[\partial_t\phi^n(t{=}1,x)\psi(1,x) - \partial_t\phi^n(t{=}0,x)\psi(0,x)]dX$$

and

$$
\begin{aligned}
< \nabla_{t,X}.(\mu^n - rq^n), \psi > &= - < \mu^n - rq^n, \nabla_{t,X}\psi > + \int_{x\in\Omega} (\mu^n - rq^n).n\psi dX \qquad (3.7)\\
&= - < \mu^n - rq^n, \nabla_{t,X}\psi > \\
&+ \int_{x\in\Omega} [(\rho^n(t{=}1, x) - ra^n(1,x))\psi(1,x) - (\rho^n(t{=}0, x) - ra^n(0,x)\psi(0,x)]dX.
\end{aligned}
$$

Hence, one may deduce the Neumann boundary conditions

$$
\begin{aligned}
r\partial_t\phi^n(1,x) &= \rho_1(x) - \rho^n(1,x) + ra^n(1,x)\\
r\partial_t\phi^n(0,x) &= \rho_0(x) - \rho^n(0,x) + ra^n(0,x)
\end{aligned}
$$

2. This step consists of finding q^n which achieves the lower bound

$$\inf_{q\in K} \{< \mu^n, \nabla_{t,X}\phi^n - q > + \tfrac{r}{2}\|\nabla_{t,X}\phi^n - q\|^2\}$$

which is equivalent to

$$\inf_{q\in K} \{< \tfrac{\mu^n}{r}, \tfrac{\mu^n}{r} > + < \tfrac{\mu^n}{r}, \nabla_{t,X}\phi^n - q > + \tfrac{1}{2} < \nabla_{t,X}\phi^n - q, \nabla_{t,X}\phi^n - q >\}$$

in other words,

$$\inf_{q\in K} \{< \tfrac{\mu^n}{r} + \nabla_{t,X}\phi^n - q, \tfrac{\mu^n}{r} + \nabla_{t,X}\phi^n - q >\}.$$

This problem corresponds to determine the projection on K of

$$(\alpha(t,x), \beta(t,x)) = (\tfrac{\mu^n}{r} + \nabla_{t,X}\phi^n)^T \in \mathbb{R}\times\mathbb{R}^d$$

which can be computed pointwise in space and time.

Indeed, for instance, let $(a(t,x), b(t,x))$ such a projection and $f(u,v) = u + \frac{1}{2}|v|^2 = 0$ the equation of the curve associated to K,

$$
\begin{cases}
(a,b) = (\alpha,\beta) + \lambda\nabla f^T_{(a,b)}\\
f(a,b) = 0.
\end{cases}
$$

This problem leads to find the smallest positive root of a third-degree-polynomial which can be efficiently performed by Cardan's method.

3.4 Presentation of the subject

The main idea is taken from [2]. Given two sequences $\rho_0(x,s)$ and $\rho_1(x,s)$, we want to determine $\forall t$, $(\rho_t(x,s), v_t(x,s))$ according to the Benamou-Brenier's formulation (3.4). There exists several ways to compute such a couple :

- ρ_0 and ρ_1 defined two sequences which can be considered as a pair of two-dimensional images. Then one can find the optimal transportation between this two images using Benamou-Brenier's algorithm.
- for each s, one may compute $\rho_t(.,s)$ the intermediate density between $\rho_0(.,s)$ and $\rho_1(.,s)$. The optimal transport is computed in one dimension.

In the first method, we allow all frames to be mixed up that is, considering a particle belonging to the frame $\rho(.,s_0)$; then this particle could move around to the frame $\rho(.,s_1)$. Whereas, in the second method, exchanges occurred frame by frame.

Section 4

Achievements

Benamou-Brenier's formulation seems more appropriate to compute an interpolating movie due to the time parameter which has been introduced. We have used the Benamou-Brenier algorithm. I was provided the implementation of this algorithm for densities defined in $\mathbb{R}^2$. The input of the algorithm are :

- number of subdivisions for each variables x,s and t,
- maximum number of iterations,
- two densities ρ_0 and ρ_1.

The output is the couple (ρ_t, m_t).

We considered several regular input data such as Gaussian sequences. Moreover, optimal transportation is defined for two sequences with the same mass. Therefore, the two sequences have to have the same total mass : $\int_{x,s} \rho_0 dxds = \int_{x,s} \rho_1 dxds$ and the same frame by frame mass: $\forall s, \int_x \rho_0(.,s)dx = \int_x \rho_1(.,s)dx$.

4.1 Optimal transportation between two images

Once we have computed the interpolation $(\rho_t(x,s), m_t(x,s))$ between the two images associated to the two sequences, one may determine on a cartesian grid the velocity field which moves around each particle of the fluid and deduce trajectories of each particle. Actually, it consists in integrating equation (3.3) by a standard 4th order Range-Kutta method.

4.2 One-dimensional transportation

As mention in 3.4, we have to compute (ρ_t, m_t) corresponding to a one-dimensional transportation (frame by frame). In this case, the trajectories are composed by several straight lines. I first implemented a method based on Benamou-Brenier algorithm.
However, this algorithm seems sophisticated compared to the result expected that is straight displacement. Indeed, (3.1) give us an easier method since, in the one-dimensional case, it is written as

$$\frac{dT}{dx}\rho_1(T(x)) = \rho_0(x).$$

To integrate this ordinary differential equation, we used an Euler's method

$$T(x_{n+1}) = T(x_n) + h\frac{\rho_0(x_n)}{\rho_1(T(x_n))}$$

with x_n the nodes of the subdivision, h its step.

This method determines the optimal application $T(x)$ according to Monge-Kantorovich formulation (3.2). On the one hand, we have verified the equivalence between Monge-Kantorovich's problem and Benamou-Brenier's problem, on the other hand, we notice that we can't directly deduce the trajectories of particles. However, concerning the Monge-Kantorovich solution, we have to approximate this optimal application. There exists several way to determine this interpolation from the Monge-Kantorovich solution $T(x)$. For instance, the McCann's interpolation yields

$$\rho_t = [(1-t)Id + tT]\#\rho_0$$

is such that

$$d_2(\rho_0, \rho_t) = t^2 d_2(\rho_0, \rho_1).$$

Moreover, it is proved, see [5], that this application is actually optimal that means for all t_0 we have the optimal application between ρ_0 and ρ_{t_0}.
Finally, trajectories are given by

$$X(t, x) = (1-t)x + tT(x).$$

which is a straight-line's equation (Figure 3).
Of course, although this algorithm is adapted to the concurrent programming (each optimal transportation may be computed independently), this method doesn't fit well with our expectations due to the frames composing the initial sequence have to interact with each other and not only with the frames of the final sequence.

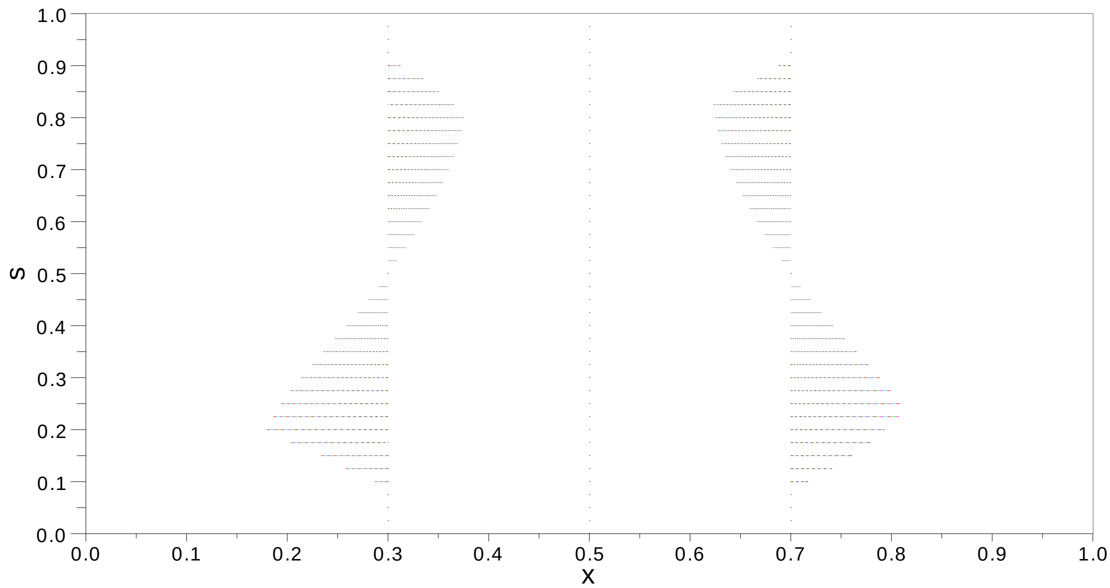

Figure 3: Trajectories of particles located at $x = 0.3$, $x = 0.5$ and $x = 0.7$ (for input data defined by section 4.1 with $f(s) = \sqrt{s}$ and $x_0 = 0.5$).

4.3 A new interpolation's method

4.3.1 Motivations

Let considered two probability densities defined in $[0, 1]^2$ by

$$\rho_0(x, s) = \frac{\sqrt{k}}{f(s)} exp(-\frac{k\pi}{f(s)^2}(x - x_0)^2)$$
$$\rho_1(x, s) = \frac{\sqrt{k}}{f(1-s)} exp(-\frac{k\pi}{f(1-s)^2}(x - x_0)^2) \tag{4.1}$$

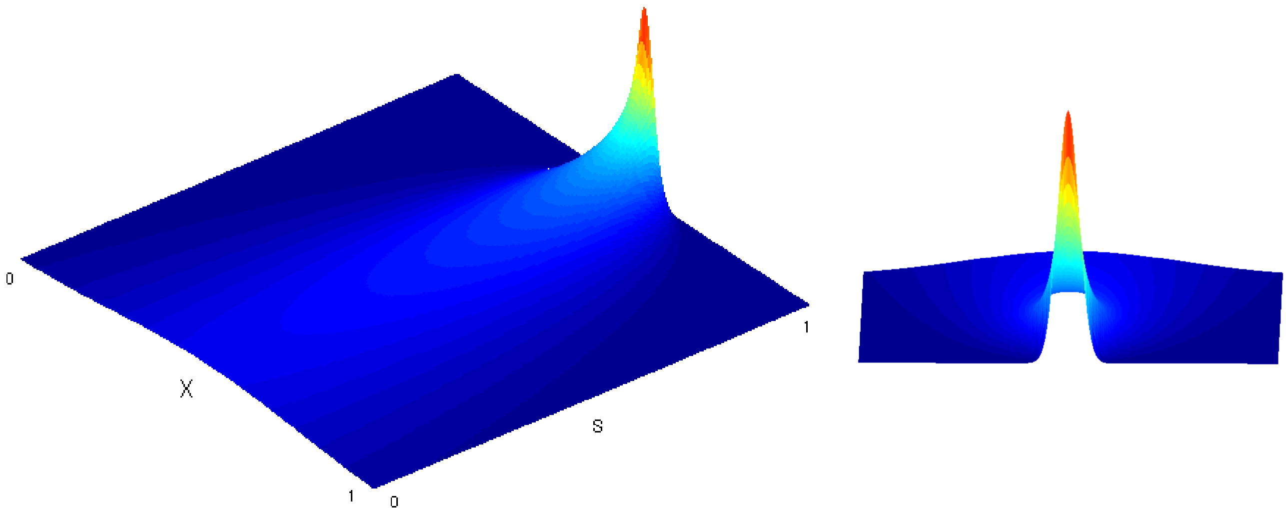

Figure 4: ρ_1 for $f(s) = \sqrt{s}$, $x_0 = 0.5$.

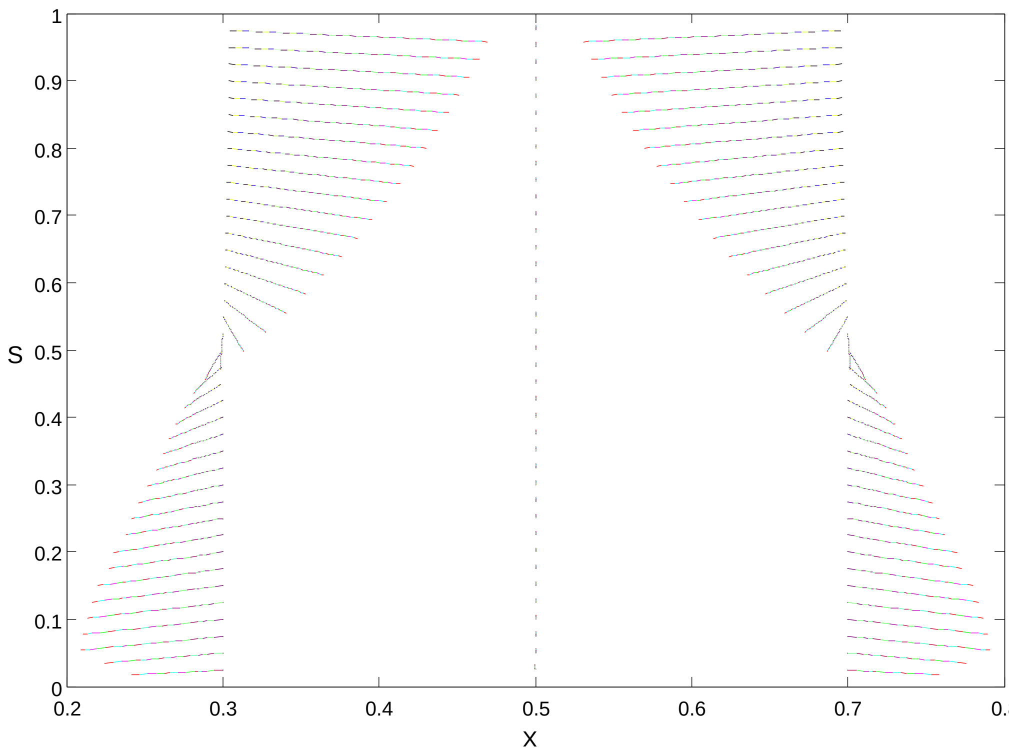

Figure 5: Trajectories of particles located at $x = 0.3$, $x = 0.5$ and $x = 0.7$

They are well-defined according to the mass conservation constraint. Typically, $f(s) = s^{\frac{1}{4}}$ for low decreasing and $f(s) = s^2$ for high decreasing.

An execution of Benamou-Brenier's algorithm is given in Appendix where some interpolating frames are illustrated. Figure 5 stands for some trajectories of particles and it stresses significant exchanges between frames.
As regards intersection trajectories located at $s \simeq 0.5$, it might makes us feel puzzled. Zooming this area, Figure 6 shows that if two segments intersect each other, then they have different colors. In fact, a path is composed by segments which have different colors. Each color/segment stands for a time interval, so particle paths don't cross in the same time.

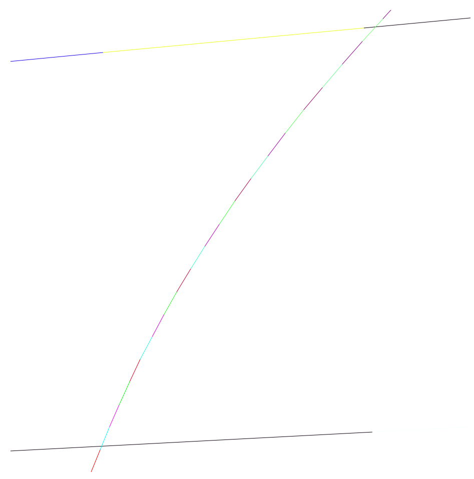

Figure 6: Intersection of trajectories.

Actually, in the framework of movie's interpolation, we want to control the motion of particles and prevent them from moving through a lot of frames.
In order to control these particles movement, we have introduced a new energy $\mathcal{E}$ to minimize. We consider the two sequences as a pair of two-dimensional images and we adapt Benamou-Brenier algorithm in order to solve our new model :

$$\begin{aligned} &minimize : \mathcal{E} = \int_{t=0}^{1} \int_{x\in\Omega} \frac{m^T A m}{\rho} dX dt \\ &subject\ to : \begin{cases} \partial_t \rho + \nabla_x . m = 0, \\ \rho(t{=}0, x) = \rho_0\ and\ \rho(t{=}1, x) = \rho_1. \end{cases} \end{aligned} \tag{4.2}$$

$$with : A = \begin{pmatrix} 1 & 0 \\ 0 & 1+\lambda \end{pmatrix} = S^T S = \begin{pmatrix} 1 & 0 \\ 0 & \sqrt{1+\lambda} \end{pmatrix} \begin{pmatrix} 1 & 0 \\ 0 & \sqrt{1+\lambda} \end{pmatrix}$$

In fact, compared to the old energy defined in (3.4),

$$\mathcal{E} = \mathcal{E}_{old} + \lambda \int_{t=0}^{1} \int_{x\in\Omega} \frac{m_2^2}{\rho} dX dt \quad with \quad m = \begin{pmatrix} m_1 \\ m_2 \end{pmatrix}$$

This equality shows that we added a penalty term on the second component of the momentum m_t and therefore, penalize movements of particles along s.

We describe several ways to solve this new problem. The first proceeds on the step 2 of the Benamou-Brenier algorithm and modify its complexity whereas the others methods provide equivalent complexity.

4.3.2 Implementation of the new model

Notations are the same as in section 3.3.
The new Lagrangian may be written as

$$L(\phi, \rho, m) = G(\phi) + \int_{t=0}^{1} \int_{x\in\Omega} \frac{m^T A m}{2\rho} dX dt - < \mu, \nabla_{t,X} \phi > . \tag{4.3}$$

Then we build an other projection space

$$\frac{m^T Am}{2\rho} = \sup_{(a,b)\in\tilde{K}} \{a(t,x)\rho(t,x) + b(t,x).m(t,x)\}$$

where $\tilde{K} = \tilde{S}K$ *and* $\tilde{S} = \left(\begin{array}{c|c} 1 & 0 \\ \hline 0 & S \end{array}\right)$.

$$\tilde{K} = \{(a,b) : ([0,1]\times[0,1]^2) \longrightarrow ([0,1]\times[0,1]^2) \mid b=(b_x,b_s),\ a + \frac{1}{2}b_x^2 + \frac{1}{2(1+\lambda)}b_s^2 \leq 0\}.$$

However, this leads to the following 5th degree polynomial equation instead of a cubic equation

$$Z^5 + (2\lambda-\alpha-1)Z^4 + \lambda(\lambda-2\alpha-2)Z^3 - (\lambda^2(\alpha+1) + \frac{\beta_x^2}{2} + (1+\lambda)\beta_s^2)Z^2 - \lambda\beta_x^2 Z - \lambda^2\frac{\beta_x^2}{2} = 0.$$

So that the complexity of the algorithm is sharply affected. Indeed, let N the number of intermediate nodes for the space interval (x), time interval (s) and the interpolation interval (t). Initially, the complexity (in term of arithmetic operations) of the step 2 was in $O(N^2)$ since we project N^2 couples $(\alpha(x,s),\beta(x,s))$ and the Cardan's method is performed in a few arithmetic operations (≤ 10). Now, our method calls a routine returning the smallest roots of a 5th degree polynomial function which can be figured out by finding the eigenvalues of the companion matrix associated to the polynomial function ($\geq 5^3$ operations per couple). So, we are computed about 5^3 more times operations per couple than the initial algorithm.

Concerning the convergence of the algorithm, our stop condition of the algorithm is either a maximal number of iterator or a tolerance on the residual. In the latter case, we choose the Hamilton-Jacobi residual given by the optimality conditions. By differentiating the Lagrangian (4.3) with respect to ρ and m, optimality conditions are

$$\begin{cases} -\frac{m^T Am}{2\rho^2} - \partial_t\phi = 0 \\ \frac{Am}{\rho} - S^{-1}\nabla_X\phi = 0. \end{cases} \tag{4.4}$$

Hence we deduce

$$\partial_t\phi + \frac{1}{2}\|A^{-2}\nabla_X\phi\|^2 = 0.$$

4.3.3 Others avantageous implementations

I have difficulty in implementing it correctly. Nevertheless, we share some clues of the idea. We do not change the projection space K. The Lagrangian defined by (4.3) may also be written as

$$\begin{aligned} L(\phi,\rho,m) &= G(\phi) + \int_{t=0}^1 \int_{x\in\Omega} [\frac{\overline{m}^T\overline{m}}{2\rho} - \rho\partial_t\phi - S^{-1}\nabla_{t,X}\phi.\overline{m}]dXdt \\ &= G(\phi) + \int_{t=0}^1 \int_{x\in\Omega} [\frac{\overline{m}^T\overline{m}}{2\rho} - < \overline{\mu}, \tilde{\nabla}_{t,X}\phi >]dXdt. \end{aligned}$$

where $\overline{m} = Sm$, $\overline{\mu} = (\rho\ \ \overline{m})^T$ and $\tilde{\nabla}_{t,X} = (\partial_t\ \ \partial_x\ \ \frac{1}{\sqrt{1+\lambda}}\partial_s)^T$.
Then, the equation solved in step 1 becomes

$$-r\tilde{\Delta}_{t,X}\phi(t,x,s) = \tilde{\nabla}_{t,X}.(\overline{\mu}(t,x,s) - rq(t,x,s))$$

where $\tilde{\Delta}_{t,X} = \tilde{\nabla}_{t,X}^T\tilde{\nabla}_{t,X}$. Here, the idea is to make a change of variable in order to obtain a "classic" Laplacian operator. Let $\phi(t,x,y) = \tilde{\phi}(t,x,\hat{s})$ where $\hat{s} = \sqrt{1+\lambda}s$, the latter equation is

$$\Delta_{t,\hat{X}}\tilde{\phi}(t,x,\hat{s}) = \nabla_{t,\hat{X}}.(\tilde{\overline{\mu}} - r\tilde{q}).$$

In the implementation, change of variable is done by changing the interval bounds on which Laplace's equation is solved.
Also, we have to take into account boundary conditions. Assume that the normal velocity is not forced to be zero on the boundaries, similarly to (3.6) and (3.7), only condition along s is modified :

$$\frac{r}{1+\lambda}\partial_s\phi^n - r\frac{1}{\sqrt{1+\lambda}}b_s + m_s = 0 \Leftrightarrow r\partial_{\hat{s}}\hat{\phi}^n = b_s - \sqrt{1+\lambda}m_s.$$

This method has the same complexity as the Benamou-Brenier algorithm since we do not change the number of subdivision's nodes but just boundary values.

4.4 Results

Our method is based on the same theoretical mathematics points, we have just changed the way to implement it. So, results (in terms of residuals, velocity field, trajectories, interpolation found) are the same for these methods.
We compute the finite sums $S_x(\lambda) = \sum_{t\in[0,1]}\sum_{X\in[0,1]^2}|v_x(t,X)|$ and $S_s(\lambda) = \sum_{t\in[0,1]}\sum_{X\in[0,1]^2}|v_s(t,X)|$ and check that $S_s(\lambda)$ is decreasing.

λ	$S_x(\lambda)$	$S_s(\lambda)$	λ	$S_x(\lambda)$	$S_s(\lambda)$
0	11.890	2.278	1	12.030	1.186
0.01	11.815	2.257	5	12.115	0.486
0.1	11.856	2.078	10	12.135	0.326

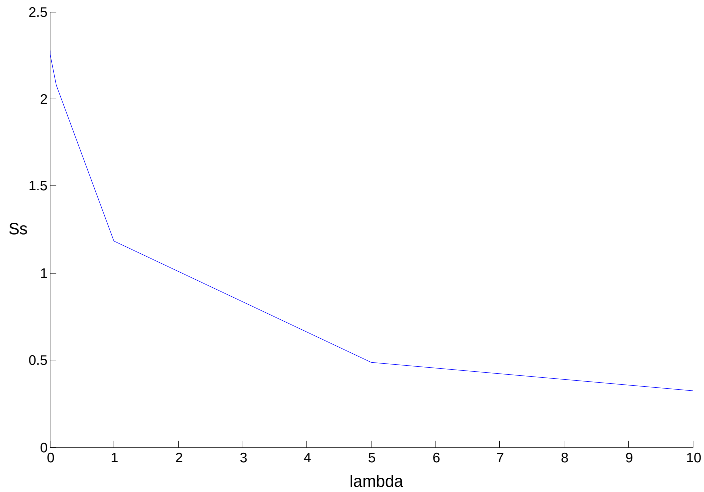

Figure 7: $S_s(\lambda)$

As λ goes to $+\infty$, we seem to converge to the one-dimensional transportation method presented in 4.2. Indeed, from optimality conditions (4.4), we deduce

$$v = A^{-1}\nabla_x\phi = \begin{pmatrix} \partial_x\phi \\ \frac{1}{1+\lambda}\partial_s\phi \end{pmatrix}.$$

As λ goes to $+\infty$ and subject to $\partial_s\phi$ is bounded, this optimality condition becomes

$$v_y \underset{\lambda\to+\infty}{\longrightarrow} = 0$$

which corresponds the one-dimensional optimal transportation.
However, algorithm's behavior for large values of λ, typically $\lambda \geq 50$ is unstable and we didn't check this result numerically.
One may compare visually Figure 5 which shows trajectories for $\lambda = 0$ and Figure 8 which corresponds to the same input data except for $\lambda = 10$.

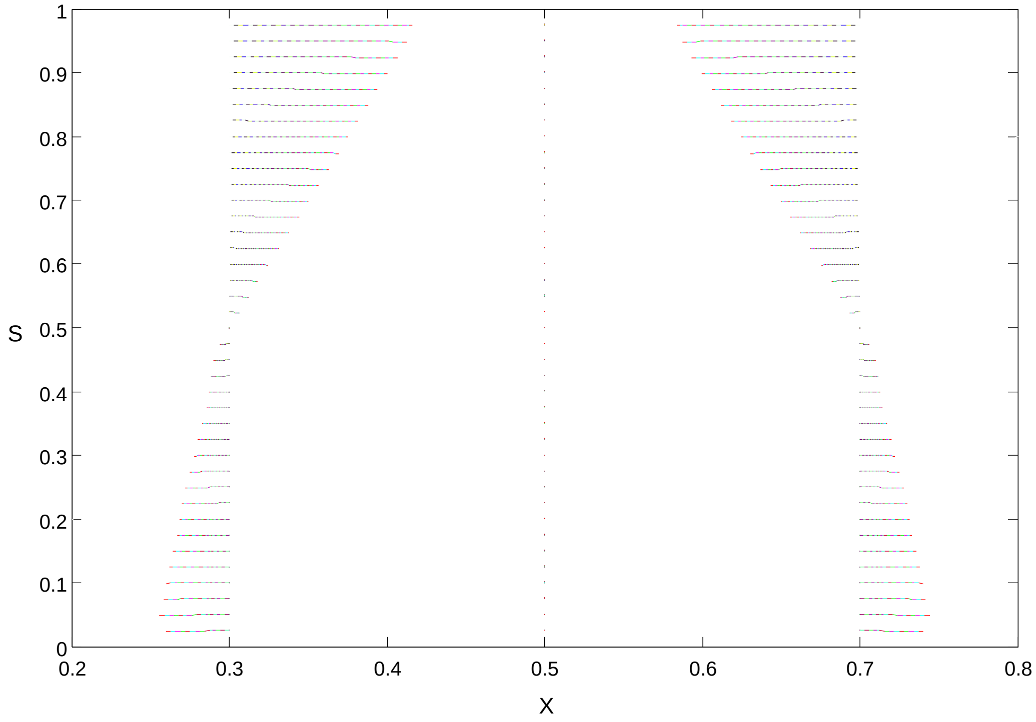

Figure 8: Visual comparisons between $\lambda = 0$ (Figure 5) and $\lambda = 10$.

Section 5

Openings

In our formulation's model (4.3), A stands for a constant diagonal matrix. It may seems interesting to consider $A(t, X)$. Indeed, we could think to control particle movements only on some areas of the fluid. Typically, in Figure 5, there is no use to apply the same penalization on all particles but for instance, we would like to proceed on the area defined by $(x, s) \in [0.25, 0.35] \times [0.4, 0.65]$ where movements along s seem the most important.
This approach would require to review each equality of the algorithm since, in our model, we use the fact that A is diagonal (so it commutes with matrices) and constant in time and space.

A theory point deals with the Brenier's polar factorisation which is intimately connected with mass transportation. This theorem (see [5]) stipulates that any nondegenerate vector-valued mapping h, that is satisfying for any small set A in $\mathbb{R}^n$, $|h^{-1}(A)| = 0$, can be rearranged into the gradient of a convex function

$$h = \nabla\psi \ o \ s$$

where s is a unique measure-preserving and ψ a convex function.
In particular, this theorem stresses that minimizers are gradients of convex functions. For the sake of our purpose, the optimal application T defined in the Monge-Kantorovich problem (3.2) may be written as a gradient of a convex function [4]

$$T = \nabla\psi.$$

So that, how do we express this factorization considering our new model with A depending on t and X ?

Section 6

Conclusion

Due to the Eulerian point of view associated to an image, optimal transportation is interpreted in a very intuitive way. This allowed us to consider the Benamou-Brenier's formulation to propose a new model aiming to favor a direction of particle paths. In particular, considering two sequences of two-dimensional images, we achieved to prevent particles from moving up/down to others frames. The implementation provided is not efficient in the sense that others solutions could have the same complexity as the Benamou-Brenier's algorithm.

Personal reviews. This internship was an opportunity to have an overview on the researcher's job and the optimal transportation theory. I really appreciate the subject : it deals with many areas of applied mathematics such as optimization, fluid mechanics, functional analysis or even image processing.
Although we have equivalence between implementing methods of our new model, I had difficulty in showing this point numerically. Moreover, I realized how difficult it was to find new perspectives. I really appreciate interactions with researchers which are necessary to develop new ideas.

References

[1] J.D. Benamou and Y. Brenier. A computational fluid mechanics solution to the monge-kantorovich mass transfer problem. *Numerische Mathematik*, 84(3):375–393, 2000.

[2] Y. Brenier. A note on deformations of 2d fluid motions using 3d born-infeld equations. *Monatshefte für Mathematik*, 142(1):113–122, 2004.

[3] M. Fortin and R. Glowinski. *Augmented Lagrangian Methods*, volume 15. Elsevier, 1983.

[4] E. Maitre. *Transport optimal, méthodes level set, applications à l'image - http://www-ljk.imag.fr/membres/Emmanuel.Maitre.*

[5] C. Villani. *Topics in optimal transportation*, volume 58. Amer Mathematical Society, 2003.

Appendix

Section 7

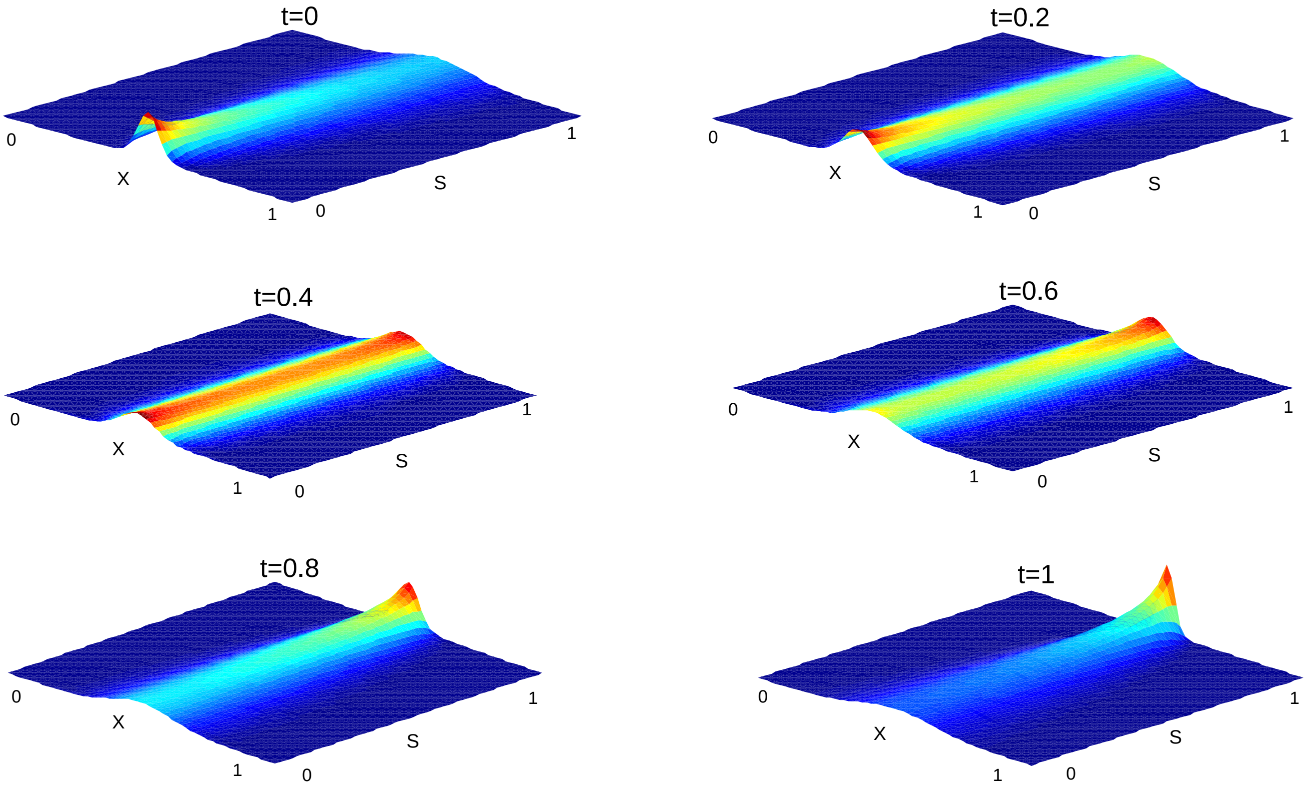

Figure 9: Interpolating frames between two gaussian densities for $t \in \{0, 0.2, 0.4, 0.6, 0.8, 1\}$ by using the 2D Benamou-Brenier's algorithm